Journal of Applied Physics

RESEARCH ARTICLE | MARCH 25 2015

On the interplay between phonon-boundary scattering and phonon-point-defect scattering in SiGe thin films

A. Iskandar; A. Abou-Khalil ; M. Kazan; W. Kassem ; S. Volz

J. Appl. Phys. 117, 125102 (2015)
https://doi.org/10.1063/1.4915948

17 April 2024 07:46:39

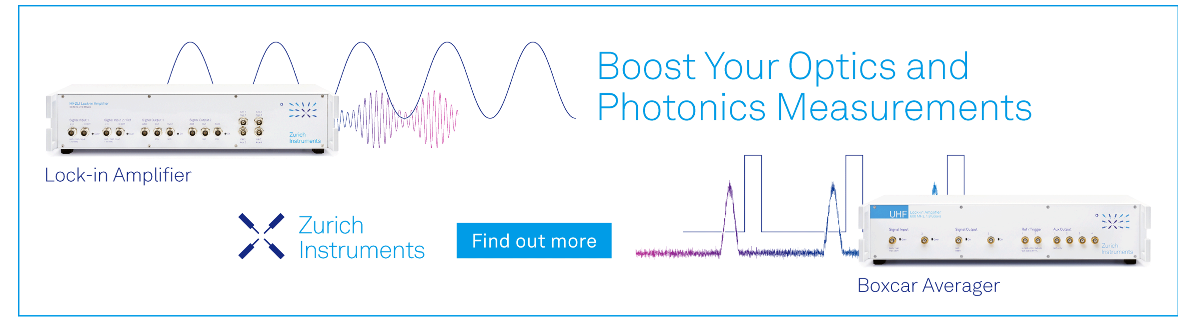

JOURNAL OF APPLIED PHYSICS **117**, 125102 (2015)

On the interplay between phonon-boundary scattering and phonon-point-defect scattering in SiGe thin films

A. Iskandar,[1] A. Abou-Khalil,[1] M. Kazan,[1] W. Kassem,[2] and S. Volz[2]
[1]*Department of Physics, American University of Beirut, P.O. Box 11-0236, Riad El-Solh, Beirut 1107-2020, Lebanon*
[2]*Laboratoire d'Energie Moleculaire et Macroscopique, Combustion CNRS UPR 288, Ecole Centrale Paris, Voie des Vignes, F-92295 Chatenay-Malabry Cedex, France*

(Received 23 September 2014; accepted 11 March 2015; published online 25 March 2015)

This paper provides theoretical understanding of the interplay between the scattering of phonons by the boundaries and point-defects in SiGe thin films. It also provides a tool for the design of SiGe-based high-efficiency thermoelectric devices. The contributions of the alloy composition, grain size, and film thickness to the phonon scattering rate are described by a model for the thermal conductivity based on the single-mode relaxation time approximation. The exact Boltzmann equation including spatial dependence of phonon distribution function is solved to yield an expression for the rate at which phonons scatter by the thin film boundaries in the presence of the other phonon scattering mechanisms. The rates at which phonons scatter via normal and resistive three-phonon processes are calculated by using perturbation theories with taking into account dispersion of confined acoustic phonons in a two dimensional structure. The vibrational parameters of the model are deduced from the dispersion of confined acoustic phonons as functions of temperature and crystallographic direction. The accuracy of the model is demonstrated with reference to recent experimental investigations regarding the thermal conductivity of single-crystal and polycrystalline SiGe films. The paper describes the strength of each of the phonon scattering mechanisms in the full temperature range. Furthermore, it predicts the alloy composition and film thickness that lead to minimum thermal conductivity in a single-crystal SiGe film, and the alloy composition and grain size that lead to minimum thermal conductivity in a polycrystalline SiGe film. *© 2015 AIP Publishing LLC*. [http://dx.doi.org/10.1063/1.4915948]

17 April 2024 07:46:39

I. INTRODUCTION

The conversion between heat flux and electricity through thermoelectric effects is attracting heightened interest due to the current need for alternative technologies to replace the shrinking supply of fossil fuel. The efficiency of a material in thermoelectric conversion is related to the dimensionless figure of merit $ZT = (\frac{S^2\sigma}{\kappa})T$, where S, σ, κ, and T are the Seebeck coefficient, electrical conductivity, thermal conductivity, and absolute temperature, respectively. Thus, a good thermoelectric material should exhibit high values for σ and S and a low value for κ. Unfortunately, nature does not provide materials with high electrical properties and low thermal properties. Therefore, efficient thermoelectric materials should be engineered. The design of a highly efficient thermoelectric system, however, has demonstrated to be a challenging task as one has to engineer a material that behaves as "phonon-glass/electron-crystal" (PGEC); that is, it would have the electrical properties of a crystalline material and thermal conductivity as low as that of an amorphous or glass-like material. It has been proposed that the increase in the electron density of states at the Fermi level along with the enhancement of the phonon scattering is the only way to attain PGEC characteristics for high efficiency thermoelectric conversion.

Several attempts have been made to enhance ZT by increasing σ and S.[1] Nevertheless, it has been found that σ and S behave oppositely when the material is doped or nanostructured.[2,3] Thus, it has been concluded that an ultra-low κ along with σ and S values of a crystalline material are key characteristics that an efficient thermoelectric material should present.[2,3] In other words, it has been concluded that the best strategy to enhance ZT is to scatter the phonons (the heat carriers) without affecting the valence electrons.

Theoretically, the lower limit of κ of a crystalline material is attained when all the phonons are scattered to reach a mean free path essentially equal to the interatomic spacing of the constituent atoms.[4] This has been attempted by scattering phonons in different frequency ranges using a variety of methods such as mass fluctuation scattering, grain-boundary scattering, and interface scattering. Alloys of silicon (Si) and germanium (Ge) have been demonstrated to be excellent candidates for high-temperature thermoelectric generation because they efficiently scatter high energy phonons and substantially reduce the material's thermal conductivity without unduly reducing the carrier mobility. As such, $ZT \approx 0.6 - 0.7$ could be realized at high temperatures in $Si_{0.3}Ge_{0.7}$.[5] The nanostructuration of SiGe also enhances the phonon scattering rate and greatly increases the thermoelectric efficiency at high temperatures. However, it is not clearly understood whether the alloy effect or the phonon-boundary scattering mechanism is more efficient in scattering the phonons and reducing the material's thermal conductivity. In fact, it has been recently reported on a peak ZT of about 1.3 at 900 °C in n-type nanostructured SiGe alloy that can be obtained due to a drastic reduction in κ caused by the

 © 2015 AIP Publishing LLC

enhanced phonon scattering by a high density of nanograin boundaries,[6,7] while other experimental studies have shown that nanosize interfaces are less efficient in scattering short wavelength phonons than point defects. Namely, it has been shown that ZT of $Si_{0.95}Ge_{0.05}$ made up of nanosized grains is similar to that of large grained $Si_{0.8}Ge_{0.2}$ alloys.[8] Furthermore, experimental measurements have shown that κ of SiGe alloys is limited by finite size effects and sample size rather than alloying,[9,10] while other studies have confirmed that the phonon scattering rate and thermal conductivities in nanosized SiGe samples are limited by alloy effects rather than boundaries effect.[11,12] A surprising ZT value of 0.95 has also been achieved in p-type polycrystalline SiGe alloys.[13] This value that is about 50% higher than the best reported record in p-type SiGe alloys[13,14] and 90% higher than what is currently used in space flight missions supports the hypothesis that boundaries are more efficient than alloying in scattering phonons.

Indeed, a complete theoretical understanding of the interplay between the intrinsic phonon scattering, the alloy scattering, and the boundary scattering in SiGe is highly desirable to explain these controversial experimental results. With such a theoretical guidance in hand one can also gain insight into the phonon heat transport in nanostructured alloy materials and rationally tailor SiGe-based highly efficient thermoelectric systems. In this paper, we tackle this issue by using an approach for the calculation of the lattice thermal conductivity in nanostructured SiGe alloys. This approach can also be used as a predictive tool to optimize the composition and structure that lead to a crystalline SiGe material with the lowest thermal conductivity.

In order to generate expressions for the rates at which phonons are scattered by the boundaries of a finite crystal in the presence of intrinsic scattering and alloy scattering mechanisms, we solve Boltzmann equation for phonons in finite crystal with taking into account the physical nature of the phonon processes and the spatial dependence of the phonon distribution function. Besides the role of static impurities in scattering phonons, we account for the modification of the dynamical matrix due to the presence of dynamical impurities. We account for the effects of surfaces by considering the contribution of surface phonons to the lattice thermal conductivity of the nanostructures under consideration. We also account for the dependence of the crystallographic orientation (which has demonstrated to be an important determinant of κ in a finite crystal[15–17]) through a directional dependent dynamical matrix. We apply the developed model to calculate κ in single-crystal and polycrystalline SiGe thin films, and we show the conditions (sample size, temperature range, alloy compositions, etc.) where κ is limited by alloy effects rather than boundaries effects, and the conditions where the finite size of the sample is the only determinant of κ. Furthermore, we demonstrate the minimum κ that can be attained in a SiGe film.

II. THEORIES

Despite the advanced atomistic approaches developed recently,[18,19] the solution of Boltzmann transport equation with a single phonon mode relaxation time approximation, and phonon scattering rates deduced from perturbation theories remains the most used approach to calculate κ in nonmetallic materials.[20–25] This is due to the fact that such an approach is flexible to include many phonon mechanisms occurring simultaneously.

The common approach to account for the phonon scattering by boundaries in Boltzmann models is to introduce a relaxation time whose expression is given by Casimir theory,[26] modified with specularity factors.[27,28] However, such an approach is physically reasonable only when the other phonon scattering mechanisms (phonon-impurity scattering, three-phonon processes, etc.) can be ignored, i.e., in highly pure crystals and at very low temperatures. In the case where interplay between the various phonon scattering processes is present, the widely used Casimir theory turns out to be physically inappropriate to describe the overall phonon scattering rate in the crystal. In that case, a more general theory for the phonon scattering rate becomes essential to predict κ especially in nanosized materials where the phonon-boundary scattering mechanism may coexist with other phonon processes over a wide temperature range. Furthermore, in the case of nanosized materials (where surface to volume ratio is not negligible), interaction takes place between the surface phonons and the volume phonons. This may lead to a significant modification in the phonon scattering rate. Indeed, such a surface effect should be described by a fundamental treatment rather than simple specularity factors.

In a previous work,[29] we have demonstrated that κ along a well-defined crystallographic orientation is given by

$$\kappa = \sum_{[hkl]} \sum_{q_{hkl}} \sum_{j} \tau_j(q_{hkl}) \bar{v}^2_{j,hkl} \frac{\left(\hbar\omega_j(q_{hkl})\right)}{k_B T^2} \times \frac{\exp\left(\frac{\hbar\omega_j(q_{hkl})}{k_B T}\right)}{\left(\exp\left(\frac{\hbar\omega_j(q_{hkl})}{k_B T} - 1\right)\right)^2} \cos\psi_{hkl}, \tag{1a}$$

where the summation runs over all the high-symmetry direction of the crystal ($\sum_{[hkl]}$), over all the phonon states in the direction $[hkl](\sum_{q_{hkl}})$, and over all the phonon branches ($\sum_j$). In Eq. (1a), $\tau_j(q_{hkl})$ denotes the total relaxation time of the phonon of wavevector $\boldsymbol{q}$ propagating in the high-symmetry direction $[hkl]$. This total relaxation time is defined as $\tau_j(q_{hkl}) = \tau_{j,C}(q_{hkl})[1 + \frac{\beta_{j,hkl}}{\tau_{j,N}(q_{hkl})}]$. Here, $\tau_{j,C}(q_{hkl})$ is a combined relaxation time of the phonon in the state q_{hkl}, and is defined as $\frac{1}{\tau_{j,C}(q_{hkl})} = \frac{1}{\tau_{j,N}(q_{hkl})} + \frac{1}{\tau_{j,R}(q_{hkl})}$ with $\tau_{j,N}(q_{hkl})$ and $\tau_{j,R}(q_{hkl})$ being the relaxation times associated with the normal and resistive processes, respectively, and $\beta_{j,hkl}$ a parameter with the dimension of a relaxation time given by[20,29]

$$\beta_{j,hkl} = \frac{\int_0^{\frac{\theta_{D,j,hkl}}{T}} dx \frac{x^4 e^x}{(e^x - 1)^2} \frac{\tau_{j,C}(q_{hkl})}{\tau_{j,N}(q_{hkl})}}{\int_0^{\frac{\theta_{D,j,hkl}}{T}} dx \frac{x^4 e^x}{(e^x - 1)^2} \frac{1}{\tau_{j,N}(q_{hkl})} \left(1 - \frac{\tau_{j,C}(q_{hkl})}{\tau_{j,N}(q_{hkl})}\right)}, \tag{1b}$$

17 April 2024 07:46:39

with x being a dimensionless parameter defined as $x = \frac{\hbar\omega(k_{hkl})}{k_B T}$. The parameter ψ_{hkl} that appears in Eq. (1a) represents the angle between the high-symmetry direction $[hkl]$ and the direction of the temperature gradient. Thus, the average thermal conductivity of the crystal is given by

$$\bar{\kappa} = \frac{1}{m}\sum_{[hkl]}\sum_{k_{hkl}}\sum_{j}\tau_j(q_{hkl})\bar{v}_{j,hkl}^2\frac{(\hbar\omega_j(q_{hkl}))}{k_B T^2} \times \frac{\exp\left(\frac{\hbar\omega_j(q_{hkl})}{k_B T}\right)}{\left(\exp\left(\frac{\hbar\omega_j(q_{hkl})}{k_B T}-1\right)\right)^2}, \quad (2)$$

where m is the number of high-symmetry directions in the crystal structure under consideration. The number of high-symmetry directions in a given crystalline structure equals the number of independent elastic constants.[30]

To account for the effects of the interaction between the surface phonons and the volume phonons, and the interplay between the phonon-boundary scattering and phonon intrinsic scattering on κ, a spatial-dependent Boltzmann equation was solved and the rates at which phonons are scattered by boundaries were described by expressions that depend on the intrinsic scattering and the strength of the interaction between the surface phonons and the volume phonons. Considering $\alpha = x$ or y, the phonon-boundary scattering rates are given by[29]

$$\frac{1}{\tau_{B,\alpha}} = \frac{\iint v_\alpha \frac{\partial \tilde{N}}{\partial \alpha}dxdy}{\iint \tilde{N}dxdy}, \quad (3)$$

where

$$\tilde{N} = \frac{R\tau}{2}\left[\left(1-\exp\left(\frac{-x(y)}{\tau v_x}\right)\right)+\left(1-\exp\left(\frac{-y(x)}{\tau v_y}\right)\right)\right], + \sigma_z\exp\left(\frac{-x(y)}{\tau v_x}\right)+\sigma_z\exp\left(\frac{-y(x)}{\tau v_y}\right) \quad (4)$$

the deviation of the phonon distribution from the equilibrium value, with $R = -v_z\frac{d\bar{N}}{dT}\frac{\partial T}{dz}$ being the negative of the rate at which phonons are delivered to a unit volume of the reciprocal space, $x(y)$ the y-dependent distance from a boundary parallel to the x axis, measured in a direction normal to the temperature gradient, and $y(x)$ the x-dependent distance from a boundary parallel to the y axis, measured in a direction normal to the temperature gradient, and σ_z the deviation of the phonon distribution due to interactions with surface phonons propagating in the direction of the phonon heat current. The rate of phonon scattering by the boundaries of a thin film of infinite length and of width l_y and thickness $l_x (l_x \prec\prec l_y)$ is given by[29]

$$\frac{1}{\tau_{B,x}} = \frac{v_x}{l_x}.\frac{\left(1-2\frac{\sigma_z}{\tau R}\right)\left(1-\exp\left(\frac{-l_x}{\tau v_x}\right)\right)}{2-\left[\sum_\alpha\frac{\tau v_\alpha}{l_\alpha}\left(1-\exp\left(\frac{-l_\alpha}{\tau v_\alpha}\right)\right)\left(1-2\frac{\sigma_z}{\tau R}\right)\right]}, \quad (5)$$

where $\alpha = x$ or y. Here, we consider that the thin film lies in the plane yz, the thickness is measured with respect to the x-axis, and the temperature gradient is along the z-axis.

As discussed in Ref. 29, the term $\frac{2\sigma_z}{\tau R}$ in Eq. (5) has all the characteristics of the phonon specularity factor t, which is usually expressed as $t = \exp\left(\frac{-16\pi^2\lambda^2\omega^2}{v^2}\right)$ with λ being the root mean square roughness at the surface.[31] Therefore, Eq. (5) can be simplified by substituting the term $\frac{2\sigma_z}{\tau R}$ by the specularity factor t.

The intrinsic phonon relaxation times in confined structures are taken as given in Ref. 32. However, in the present paper, the possible decay of the volume phonons into surface phonons is accounted for.

The phonon relaxation time associated with the scattering of phonons at state q_{hkl} by static impurities in alloy systems is expressed as[33]

$$\tau_{I,j}^{-1}(q_{hkl}) = \frac{\Gamma_{md,j,hkl}\Omega}{4\pi v_{j,hkl}^3}\omega^4(q_{hkl}), \quad (6a)$$

where Ω is the volume per atom and Γ_{md} the mass-fluctuation coefficient defined as

$$\Gamma_{md,j,hkl} = \sum_i f_i\left[\left(\frac{\Delta M_i}{M}\right)^2 + 2\left(\frac{\Delta g_i}{g} - 6.4\gamma_{j,hkl}\frac{\Delta\delta_i}{\delta}\right)^2\right]. \quad (6b)$$

Here, f_i is the concentration of the ith element in the alloy, δ_i the atomic radius of the ith element in the alloy, δ the radius of an atom in the virtual crystal, g_i an average stiffness constant of the nearest-neighbor bonds from the impurity to the host lattice, g the average stiffness constant for the host atoms, $\Delta g_i = g_i - g$, $\Delta\delta_i = \delta_i - \delta$, and $\gamma_{j,hkl}$ the Grüneisen parameter of the phonon branch j in the direction $[hkl]$.

For the calculation of the in-plane κ in polycrystalline thin films, one has to account for the existence of boundaries in the direction along which the phonon heat current is directed. This can be made possible by noting that in the plane of the thin film, every grain experiences the same heat flux, but different temperature gradient due to the thermal resistances of the boundaries.[29] Thus, the effect of grain boundaries in the direction of the heat current can be accounted for by simply considering that these boundaries add resistances to the intrinsic resistance of the film without boundaries. Therefore, the in-plane κ of a polycrystalline thin film can be expressed as[29]

$$R_z = \sum_{i=2}^{n_z} R_1 + R_i + R_{B,(i-1)i}, \quad (7)$$

where R_1 is the resistance of the first grain, R_i the resistance of the ith grain, $R_{B,(i-1)i}$ the resistance of the boundary between the grain $(i-1)$ and the ith grain, and n_z the average number of grains in the z direction (the direction along which the heat current is directed). Considering L_z the sample dimension in the z direction, l the average grain size in the z direction, $\bar{R}_B$ an average boundary thermal resistance, and $\bar{n}_z$ equals $\frac{L_z}{l}$ rounded to the nearest integer, the in-plane κ in polycrystalline thin film can be written as[29]

17 April 2024 07:46:39

$$\kappa = \frac{L_z}{\bar{n}_z\left[\frac{l}{\kappa_{single-crystal}} + \bar{R}_B\right] - \bar{R}_B}, \tag{8}$$

where $\kappa_{single-crystal}$ is the intrinsic thermal conductivity of the film without boundaries. The thermal resistance of a boundary between two different materials is the inverse of the boundary thermal conductance TC, which is defined as[34]

$$TC = \frac{1}{2}\sum_j \sum_{\mathbf{q}} \frac{1}{k_B T^2}\hbar^2\omega_j^2(\mathbf{q})v_j(\mathbf{q}) \times \frac{\exp\left(\frac{\hbar\omega_j(\mathbf{q})}{k_B T}\right)}{\left[\exp\left(\frac{\hbar\omega_j(\mathbf{q})}{k_B T}\right) - 1\right]^2}\Gamma_j(\mathbf{q}), \tag{9}$$

where $\Gamma_j(\mathbf{q})$ is the probability for a phonon of polarization j and wavevector $\boldsymbol{q}$ to transmit specularly or diffusively across the boundary. It can be shown that the transmission probability across a boundary between two grains of the same material is independent of the orientations of the grains at both sides of the boundary,[29,35,36] and of magnitude given by

$$\Gamma_j(\mathbf{q}) = \Gamma = \bar{\mu} + \frac{1-t}{2}, \tag{10}$$

where $\bar{\mu}$ is an average specular transmission probability equaling to $\frac{4t}{2m}\left(\frac{m}{4} + \sum_{[h'l'k'] \neq [hkl]}^{[hkl]} \frac{\bar{v}_{hkl}\bar{v}_{h'k'l'}}{(\bar{v}_{hkl}+\bar{v}_{h'k'l'})^2}\right)$ and t a specularity factor equaling to $\frac{2\sigma_z}{\tau R}$.

We note that at small spatial scales (smaller than the phonon coherence length),[37] the phonon may not feel the interface separating two materials, and propagate ballistically without being scattered at the interface. Such a phonon mechanism is known as the coherent phonon transport mode. Basically, such a phonon mechanism might be encountered at very clean interfaces. When irregularities are present at the interfaces, the phonons scatter regardless the size of the material where they come from or going to because these irregularities become the only determinant of the phonon mean free path and coherence length. Typically, in granular and polycrystalline materials of randomly oriented grains, the grain boundary presents an important amount of irregularity. Therefore, the assumption that the phonon transport from grain to grain is incoherent and the phonons scatter at the grain boundary irrespectively to the average grain size is reasonably justified.

III. COMPUTATIONAL DETAILS

All the parameters in Eqs. (1) and (2) are calculated from elasticity theory that treats the thin film as a block of matter without invoking any interatomic potentials. The only input parameter is the phonon group velocity in the bulk material. The advantage of this technique is that it has no size limitation, and can be reliably applied to verify the trend of physical properties when the size of the material goes from the nanoscale to infinity. The "allowed" wavevectors, $\boldsymbol{q}$, are considered to be the ones that satisfy Ortavy criterion[38]

$$|\mathbf{q}|^2 = \pi^2\left(\frac{n_1^2}{l_1^2} + \frac{n_2^2}{l_2^2} + \frac{n_3^2}{l_3^2}\right), \tag{11}$$

where l_1, l_2, and l_3 are the dimensions of the sample, and n_1, n_2, and n_3 are positive integers. These integers cannot run to infinity. The number of modes (or the number of atoms in the sample) sets their limiting values. We derive all the allowed wavevectors by following Ortavy criterion and we carry out the calculation of the lattice thermal conductivity for all the allowed wavevectors.

The eigenfrequencies of the acoustic phonon modes confined in thin films can be derived from acoustics.[39] The main difference between the confined phonon modes and the phonon modes in infinite crystals is that the x component of the confined mode wavevector, q_x, takes discrete set of values at each particular in-plane wavevector $\boldsymbol{q}$. The theory describing the confinement of the acoustic phonon modes and the corresponding relative displacement vector components is detailed in Ref. 40. In the present paper, we only report the basic elements required for the computation of the eigenfrequencies $\omega_j(q)$ of the confined acoustic phonon modes in thin films. The dispersion relation for shear modes in the direction $[h,k,l]$ is given by[40]

$$\omega_{j,hkl} = v_{hkl,T}\sqrt{q_{x,j}^2 + q^2}, \tag{12}$$

where $v_{hkl,T}$ is the transverse phonon group velocity in the direction $[h,k,l]$ and $q_{x,j} = \frac{\pi j}{l}$ is the x component of the wavevector that is quantized based on the assumption that an integer number of half wavelengths fits in a semiconductor slab of thickness l.

The dispersion relation for dilatational modes in the direction $[h,k,l]$ is given by[40]

$$\omega_{j,hkl} = v_{hkl,L}\sqrt{q^2 + q_{l,j}^2} = v_{hkl,T}\sqrt{q^2 + q_{t,j}^2}, \tag{13}$$

where $v_{hkl,L}$ is the bulk longitudinal phonon group velocity in the direction $[h,k,l]$ and the parameters $q_{l,j}$ and $q_{t,j}$ are the solutions of the system of two algebraic equations

$$\frac{\tan\left(\frac{q_t l}{2}\right)}{\tan\left(\frac{q_l l}{2}\right)} = -\frac{4q^2 q_l q_t}{\left(q^2 - q_t^2\right)^2} \quad \text{and} \quad v_{hkl,L}^2\left(q^2 + q_l^2\right) = v_{hkl,T}^2\left(q^2 + q_t^2\right). \tag{14}$$

This system of equations has many solutions for q_l and q_t at each in-plane wavevector $\boldsymbol{q}$. Each solution is labeled by an index (or branch number) j. These solutions are either real or pure imaginary depending on $\boldsymbol{q}$ and j. The real solutions result in phonon branches describing the eigenfrequencies of volume modes, whereas the pure imaginary solutions result in phonon branches describing the eigenfrequencies of evanescent phonon modes localized at the surface. Such modes are known as surface phonon modes.

17 April 2024 07:46:39

The dispersion relation for the flexural modes (or transverse modes) can be obtained from Eq. (14) by simply exchanging $q_{l,j}$ and $q_{t,j}$ because by this way the force generating the elastic wave makes the particles of the medium moving perpendicularly to the direction of propagation of the wave. This gives many new solutions for q_l and q_t at each in-plane wavevector of flexural modes. The solutions q_l and q_t for flexural modes may also be either real or pure imaginary for a given set of $\boldsymbol{q}$ and j. Thus, the solutions for flexural modes also result in phonon branches describing the frequencies of volume modes, and phonon branches describing the eigenfrequencies of localized surface modes. It is worth noting that we consider only the real eigenfrequencies of the imaginary $q_{l,j}$ and $q_{t,j}$ as the eigenfrequencies of the surface modes. We do not account for any imaginary eigenfrequencies because the SiGe lattice is stable in the temperature range investigated.

The theory of elasticity predict in the folded Brillouin zone of a nanostructured material a large number of phonon branches that flatten out as the frequency increases. Since the phonon group velocity corresponding to a given phonon branch is determined only by the slope of the phonon branch, the high frequency phonon branches have negligible contribution to the thermal conductivity. Therefore, although the elasticity theory predicts a large number of phonon branches exceeding the cutoff frequency of the bulk material, it can accurately predict the thermal conductivity of nanostructures because the high frequency branches have very low group velocities, and consequently have almost no effect on the lattice thermal conductivity.

The average phonon group velocity in nanostructures has been intensively investigated within the continuum medium approximation.[32,41–44] However, since the model developed in the present work assumes discrete lattice wavevectors, one should account for the fact that only the confined modes of small wavevectors are excited at low temperatures and almost all the modes are excited at high temperatures. Thus, one has to express the phonon group velocity as a function of temperature. To do so, we write the temperature-dependent average group velocity for the confined acoustic phonon that corresponds to the branch j in the direction $[h,k,l]$ as given in Ref. 45.

$$\bar{v}_{j,hkl} = \frac{\sum_{q_{hkl}} v_{j,q_{hkl}}.\bar{N}_j(q_{hkl})}{\sum_{q_{hkl}} \bar{N}_j(q_{hkl})}, \tag{15}$$

where $v_{j,q_{hkl}}$ is the derivative of the jth phonon branch in the direction $[h,k,l]$ at q_{hkl} and $\bar{N}_j(q_{hkl})$ the equilibrium phonon occupation of the state q_{hkl}.

The introduction of the parameter β (that is expressed in Eq. (1b)) simplifies Boltzmann equation when the effects of the normal processes, which drag the crystal momentum back and forth between the normal modes, are accounted for.[20] Nevertheless, the Debye-temperature should be temperature-dependent in order for β to provide a solution for Boltzmann equation over a wide temperature range.[46] To express the Debye-temperature as a function of temperature, we equate the specific heat for the jth branch in the direction $[h,k,l]$ calculated with the discrete phonon wavevectors to the Debye approximation of the specific heat

$$C_{j,hkl} = k_B \sum_{q_{hkl}} \frac{\left(\frac{\hbar\omega_j(q_{hkl})}{2k_BT}\right)^2}{\sinh\left(\frac{\hbar\omega_j(q_{hkl})}{2k_BT}\right)} = 3rN_ck_B\left(\frac{T}{\theta_{D,j,hkl}}\right)^3 \int_0^{\frac{\theta_{D,j,hkl}}{T}} \frac{x^4e^x}{(e^x-1)^2}dx, \tag{16}$$

and consider the resulting equation as an expression for the Debye-temperature for the jth branch in the direction $[h,k,l]$. By this way, we obtain the theoretical dependence of the Debye-temperature for the jth branch in the direction $[h,k,l]$ on temperature. In Eq. (16), r denotes the number of atoms per unit cell and N_c the number of unit cells in the crystal.

The derivation of the temperature-dependent Grüneisen parameter $\gamma_{j,hkl}$ that appears in the expressions of the relaxation time associated with the interaction of phonons at state q_{hkl} with static impurities in alloys (see Eq. (6)) and the relaxation time associated with the intrinsic scattering of confined phonons (see Ref. 32) is carried out by assuming that the contribution from each single mode Grüneisen parameter $\gamma_j(q_{hkl})$ to the overall Grüneisen parameter $\gamma_{j,hkl}$ is set by its contribution to the specific heat $C_{j,hkl}$ as

$$\gamma_{j,hkl} = \frac{\sum_{q_{hkl}} \gamma_j(q_{hkl}) \times C_{j,hkl}}{\sum_{q_{hkl}} C_{j,hkl}}, \tag{17}$$

then calculating the single mode Grüneisen parameter $\gamma_j(q_{hkl})$ from its definition $\gamma_j(q_{hkl}) = \frac{-\Omega}{\omega_j(q_{hkl})}\frac{\partial\omega_j(q_{hkl})}{\partial\Omega}$. At this point, all the ingredients in Eqs. (1)–(10) are found, so the numerical calculation of the thermal conductivity in single-crystal and polycrystalline thin films is made possible.

IV. RESULTS AND DISCUSSION

In order to visualize the effect of the alloy composition on the dynamical matrix of a nanosized SiGe film, we have plotted the eigenfrequencies of phonon modes in 10 nm thick SiGe slab oriented in the [111] direction for several alloy compositions. The eigenfrequencies of the shear modes, dilatational modes, flexural modes, and surface modes are shown in Figs. 1, 2, 3, and 4, respectively, together with the corresponding Debye-like acoustic phonon branch in infinite crystal. As can be noticed, the magnitudes of the eigenfrequencies and phonon group velocities decrease with increasing the alloy composition. Thus, the alloy has a two-fold effect on κ. It reduces κ due to the enhancement of the rate at which phonons are scattered by static impurities, and due to the reduction in the phonons eigenfrequencies and group velocities that are key determinants of κ. The model developed in the present paper accounts for both effects.

In order to verify its accuracy, we have used the developed model to reproduce previously reported experimentally measured κ in single-crystals and polycrystalline thin films of SiGe. Namely, the model was applied to reproduce the

17 April 2024 07:46:39

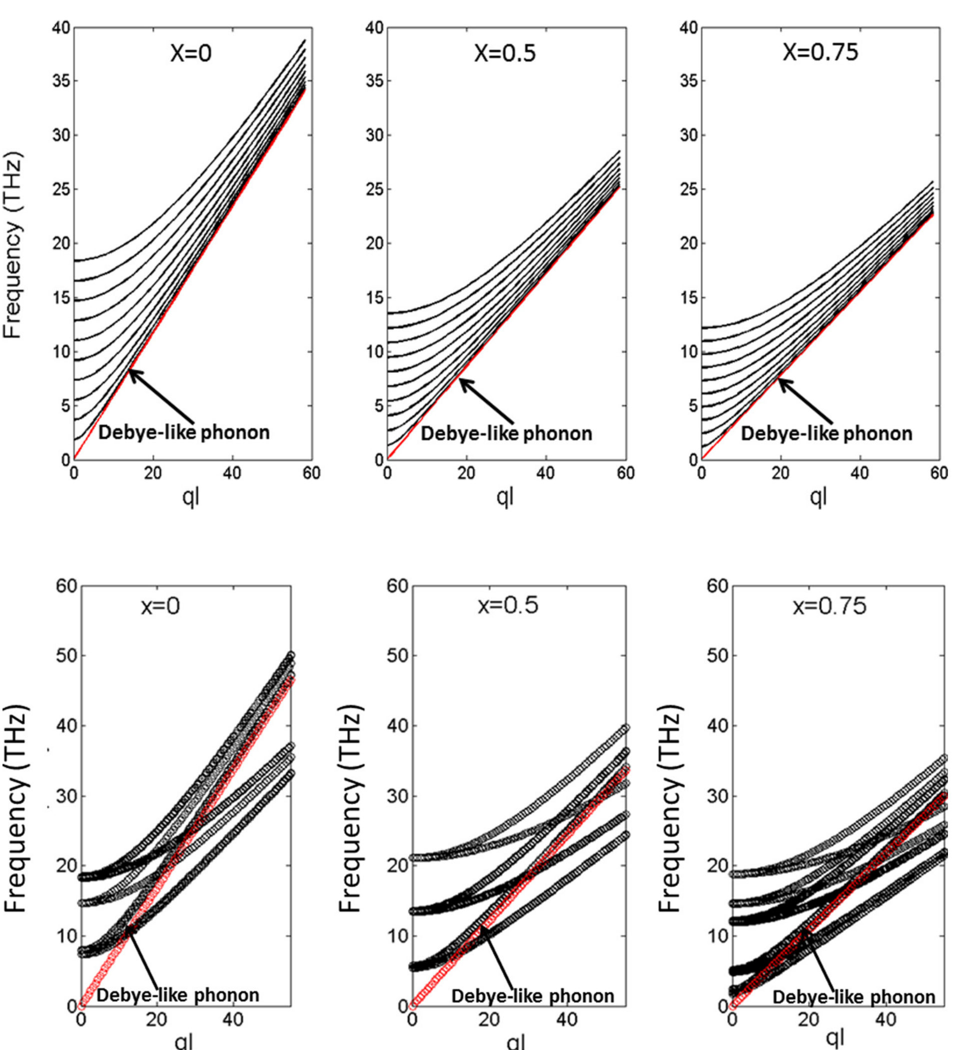

FIG. 1. Eigenfrequencies of shear acoustic modes in 10 nm thick SiGe slab oriented in the [111] direction for several alloy compositions. The red line shows the corresponding Debye-like acoustic phonon branch in infinite crystal.

FIG. 2. Eigenfrequencies of dilatational acoustic modes in 10 nm thick SiGe slab oriented in the [111] direction for several alloy compositions. The red line shows the corresponding Debye-like acoustic phonon branch in infinite crystal.

measurements of Cahill *et al*. on epitaxial layers of dilute SiGe alloy,[47] the measurements of Cheaito *et al*. on SiGe alloy single-crystal thin films,[9] and the measurements of Zhu *et al*. on nanograined SiGe samples.[8] For the calculation of κ in single-crystal thin films, the actual dimensions of the measured film were used as input parameters. However, for the calculation of κ in polycrystalline thin films, the actual dimensions of the measured film and constituent grains were used as input parameters, and the *rms* roughness λ at the grain boundaries has been adjusted until best agreement

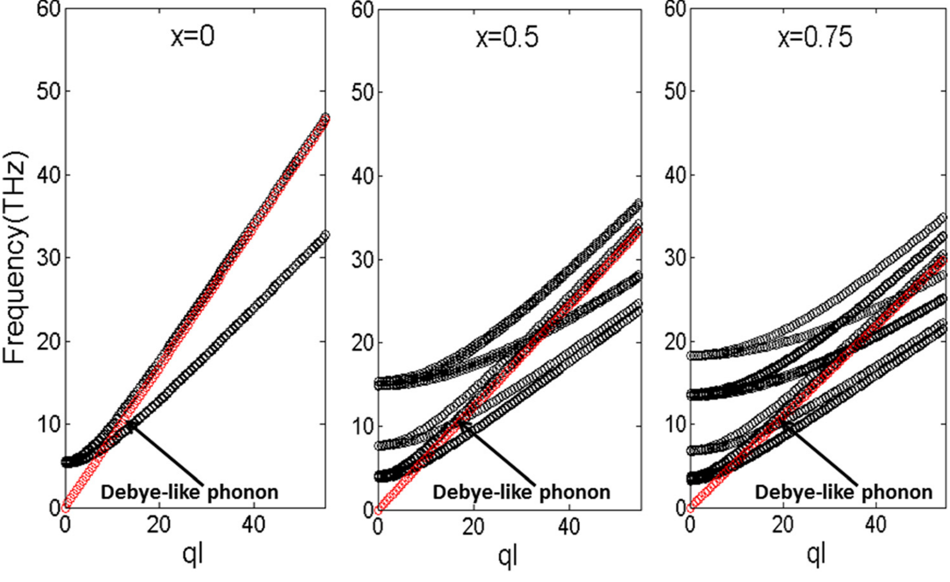

FIG. 3. Eigenfrequencies of flexural acoustic modes in 10 nm thick SiGe slab oriented in the [111] direction for several alloy compositions. The red line shows the corresponding Debye-like acoustic phonon branch in infinite crystal.

17 April 2024 07:46:39

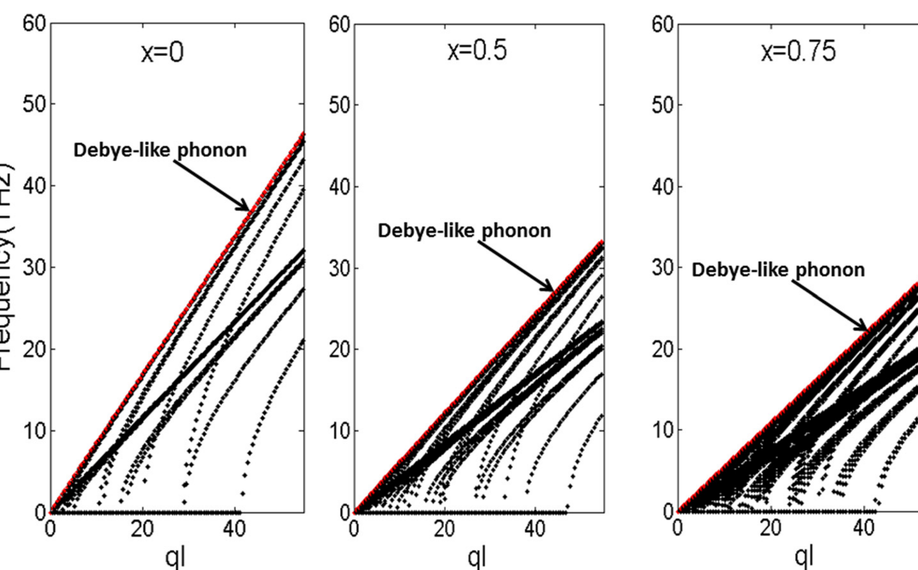

FIG. 4. Eigenfrequencies of surface acoustic modes in 10 nm thick SiGe slab oriented in the [111] direction for several alloy compositions. The red line shows the corresponding Debye-like acoustic phonon branch in infinite crystal.

between the theoretical and experimental curves was obtained. The theoretical and experimental curves are shown together in Fig. 5. The excellent agreement between calculated and measured κ reveals the importance of all the physical mechanisms involved and clearly demonstrates the predictive power and wide scope of the developed model.

An important conclusion can be drawn from Fig. 5. While the thermal conductivity of 200 and 400 nm thick single-crystal $Si_{0.8}Ge_{0.2}$ films tends to be at low temperatures greater than the thermal conductivity of polycrystalline $Si_{0.99}Ge_{0.01}$ films of 20 nm average grain size, the thermal conductivity of the polycrystalline films exceeds the thermal conductivity of the single-crystal films at high temperatures. This clearly demonstrates that the phonon scattering by grain boundaries is the dominant phonon scattering mechanism at low temperatures, whereas the phonon scattering by impurities is the dominant phonon scattering mechanism at high temperatures.

For the sake of further verification of the accuracy of the model, we have calculated the frequency-dependent intrinsic phonon relaxation times of the acoustic longitudinal phonon branch in bulk Si, and compared them to those obtained from first principles calculations.[48] The results are shown in Fig. 6. The relaxation time associated with the normal phonon scattering mechanism as obtained from the present model agrees well with that calculated by using first principles approaches. Nevertheless, the relaxation time associated with the Umklapp phonon scattering mechanism as obtained from the present model agrees with that obtained from first principles calculations only at low frequencies. This may be due to the fact that the continuum medium approximation breaks down at high frequencies. However, this discrepancy does not make the model presented in this work questionable because the intrinsic thermal conductivity of the materials is determined mainly by the low-frequency acoustic phonons due to their lower scattering rates.

We have also used the developed model to calculate the dependence of alloy composition on the thermal conductivity of SiGe at high temperatures. The obtained theoretical results are plotted in Fig. 7 together with previously reported experimental results.[49] The good agreement between the theoretical and experimental curves at all the temperatures

17 April 2024 07:46:39

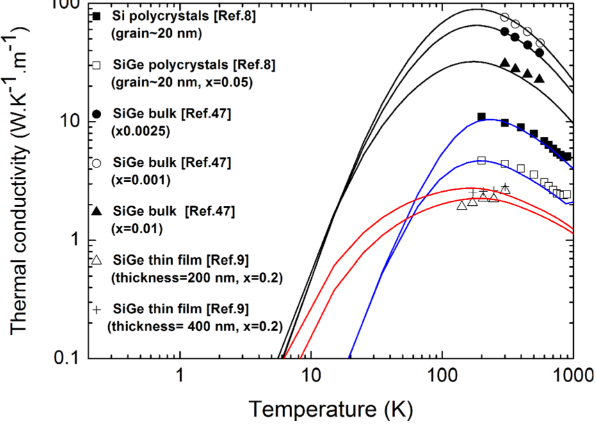

FIG. 5. Effects of alloy composition, film thickness, and grain size on the thermal conductivity of single-crystal and polycrystalline SiGe films. The symbols present previously reported experimental data. The solid lines present theoretical results obtained from the model described in the present paper.

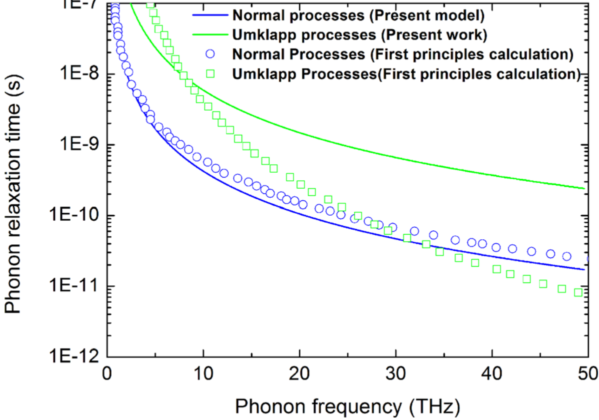

FIG. 6. Frequency-dependent phonon relaxation times of the longitudinal acoustic phonon branch in Si associated with normal and Umklapp scattering mechanisms. The lines indicate the results obtained from the model presented in this work. The symbols indicate the results obtained from first principles calculations (Ref. 48).

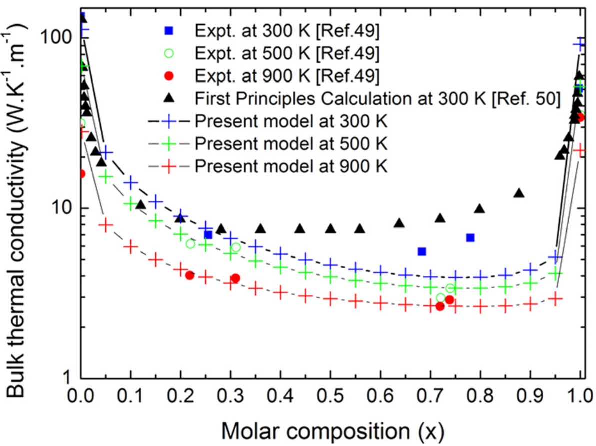

FIG. 7. Dependence of alloy composition on the thermal conductivity in SiGe at 300, 500, and 900 K. Symbols indicate previously reported experimental results. Solid lines show theoretical results obtained from the model developed in the present paper.

considered clearly demonstrates the capability of the developed model to account for the interplay between the harmonic intrinsic scattering and the anharmonic alloy scattering. It is also worth noting that the results obtained from the developed model agree with those obtained from first principles calculation,[50] which demonstrated that an addition of as little as 12% Ge is sufficient to reduce the room temperature thermal conductivity to around the minimum value achievable through alloying.

In order to investigate in a systematic way the interplay between the alloy effect and the size effect, we have plotted a mesh describing the variation of κ with the alloy composition and single-crystal film thickness at several temperatures in the three high-symmetry directions, and a mesh describing the variation of κ with the alloy composition and average grain size in a polycrystalline film at several temperatures. The three-dimensional plot describing the variation of κ with the alloy composition and single-crystal film thickness is shown in Fig. 8. Along the three high-symmetry directions, at very low temperatures (around 5 K), where the intrinsic phonon scattering mechanism is almost absent ($\tau \rightarrow 0$), κ increases as both film thickness and Ge content increase. This is due to the fact that the phonon-boundary scattering rate (Eq. (5)), which is the only determinant of κ at very low temperatures, takes the form $\frac{1}{\tau_B} = \frac{v}{l}$, and consequently it increases as the phonon group velocity increases and the film thickness decreases. At higher temperatures (around 50 K), where the phonon intrinsic scattering mechanisms partially contribute to the determination of κ, κ drops rapidly as the alloy composition attains 0.15. On the other hand, κ increases as the film thickness increases independently of the Ge content. However, at temperatures exceeding the room temperature, the effect of film thickness diminishes and κ of SiGe becomes almost limited by alloying. According to the results in Fig. 8, a 5 nm thick (100)-oriented single-crystal $Si_{0.42}Ge_{0.58}$ film reaches at room temperature a κ value as low as 0.54 W K^{-1} m^{-1}, which is a value smaller than that of κ of amorphous or glass-like materials.[51–53] Consequently, 5 nm thick (100)-oriented single-crystal $Si_{0.42}Ge_{0.58}$ film can be considered as a potential PGEC material for SiGe-based high-efficiency thermoelectric devices operating at room temperature.

The variation of κ with the alloy composition and grain size is shown in Fig. 9. At low temperatures, the alloy composition and grain size contribute equally to the phonon scattering and determination of κ. However, as the temperature increases, the alloy effect starts to dominate that of the grain size. At high temperatures, the effect of the grain size on κ becomes negligible compared to that of the alloy composition. The highest phonon scattering rate at room temperature in polycrystalline SiGe films can be reached with a grain size as small as 5 nm and a Ge molar composition of 0.8. Such polycrystalline SiGe film characteristics result in a κ value of 1.83 W K^{-1} m^{-1}, which is almost three times greater than the minimum κ that can be reached in single-crystal SiGe thin films. Thus, these results add support to the hypothesis that at temperatures greater than some tens of degrees Kelvin, the alloy is more efficient than boundary, and the grain boundary

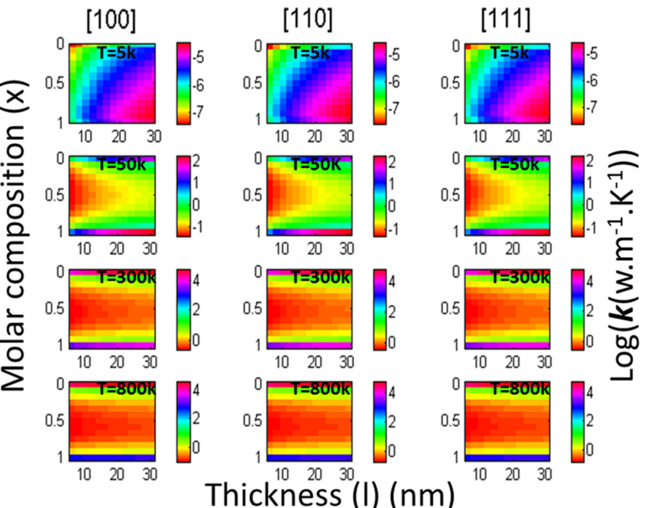

FIG. 8. Thermal conductivity of single-crystal SiGe thin film versus alloy composition and film thickness.

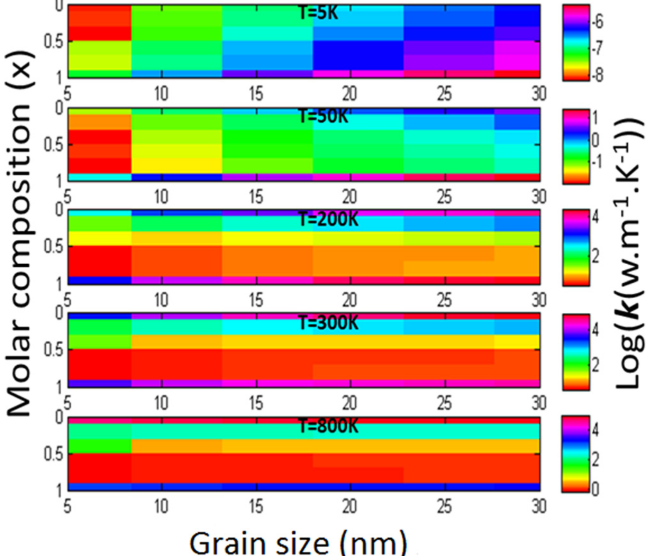

FIG. 9. Thermal conductivity of polycrystalline SiGe thin film versus alloy composition and grain size.

17 April 2024 07:46:39

is less efficient than the film boundary in scattering phonons. Consequently, single-crystal $Si_{0.42}Ge_{0.58}$ ultrathin film would be a potential material for a new generation of high-efficiency room temperature thermoelectric devices.

V. CONCLUSION

Exact Boltzmann transport equation with spatial dependence of the phonon distribution function has been solved with taking into account dispersion of confined phonon modes in nanosized films to deduce the thermal conductivity in single-crystal and polycrystalline SiGe thin films. The rates at which phonons scatter via normal and resistive processes have been derived by using perturbation theories. The vibration parameters have been introduced in Boltzmann equation as functions of temperature and crystallographic direction to obtain accurate thermal conductivity values in the full temperature range. The accuracy of the model has been clearly demonstrated with respect to previously reported experimental measurements regarding the effect of alloy on the thermal conductivity of bulk SiGe materials, the effects of alloy composition and film thickness on the thermal conductivity of single-crystal thin SiGe films, and the effect of alloy composition and grain size on the thermal conductivity of polycrystalline SiGe films. Then, the model has been used to determine at each temperature the strength of each of the phonon scattering processes. As a result, we have determined the alloy composition and film thickness that lead to the minimum thermal conductivity in single-crystal thin SiGe films, and the alloy composition and grain size that lead to the minimum thermal conductivity in polycrystalline SiGe films. Furthermore, we have demonstrated that a single-crystal thin film with specific alloy composition and thickness might attain the "phonon-glass/electron-crystal" characteristics, which are the key requirements for a new generation of high-efficiency thermoelectric devices.

ACKNOWLEDGMENTS

A.I. and M.K. would like to acknowledge the financial support by the National Council for Scientific Research (CNRS-Lebanon) and Munib and Angela Masri Institute of Energy and Natural Resources.

[1] A. F. Ioffe, *Semiconductor Thermoelements and Thermoelectric Cooling* (Infosearch, London, 1957).
[2] G. A. Slack, in *CRC Handbook of Thermoelectrics*, edited by D. M. Rowe (CRC Press, Boca Raton, FL, 1995).
[3] D. M. Rowe, in *Thermoelectrics Handbook: Macro to Nano*, edited by D. M. Rowe (CRC Press, Boca Raton, FL, 2006).
[4] G. A. Slack, in *Solid State Physics*, edited by F. Seitz, D. Turnbull, and E. Ehrenreich (Academic Press, New York, 1979), Vol. 34.
[5] C. Wood, Rep. Prog. Phys. **51**, 459 (1988).
[6] X. W. Wang, H. Lee, Y. C. Lan, G. H. Zhu, G. Joshi, D. Z. Wang, J. Yang, A. J. Muto, M. Y. Tang, J. Klatsky, S. Song, M. S. Dresselhaus, G. Chen, and Z. F. Ren, Appl. Phys. Lett. **93**, 193121 (2008).
[7] D. M. Rowe, L. W. Fu, and S. G. K. Williams, J. Appl. Phys. **73**, 4683 (1993).
[8] G. H. Zhu, H. Lee, Y. C. Lan, X. W. Wang, G. Joshi, D. Z. Wang, J. Yang, D. Vashaee, H. Guilbert, A. Pillitteri, M. S. Dresselhaus, G. Chen, and Z. F. Ren, Phys. Rev. Lett. **102**, 196803 (2009).
[9] R. Cheaito, J. C. Duda, T. E. Beechem, K. Hattar, J. F. Ihlefeld, D. L. Medlin, M. A. Rodriguez, M. J. Campion, E. S. Piekos, and P. E. Hopkins, Phys. Rev. Lett. **109**, 195901 (2012).
[10] L. Yin, E. K. Lee, J. W. Lee, D. Whang, B. L. Choi, and C. Yu, Appl. Phys. Lett. **101**, 043114 (2012).
[11] H. Kim, I. Kim, H.-J. Choi, and W. Kim, Appl. Phys. Lett. **96**, 233106 (2010).
[12] Z. Wang and N. Mingo, Appl. Phys. Lett. **97**, 101903 (2010).
[13] G. Joshi, H. Lee, Y. Lan, X. Wang, G. Zhu, D. Wang, R. W. Gould, D. C. Cuff, M. Y. Tang, M. S. Dresselhaus, G. Chen, and Z. Ren, Nano Lett. **8**, 4670 (2008).
[14] J. P. Dismukes, L. Ekstrom, E. F. Steigmeier, I. Kudman, and D. S. Beers, J. Appl. Phys. **35**, 2899 (1964).
[15] C. B. Vining, W. Laskow, J. O. Hanson, V. D. Beck, and P. D. Gorsuch, J. Appl. Phys. **69**, 4333 (1991).
[16] W. Li and N. Mingo, J. Appl. Phys. **114**, 054307 (2013).
[17] J. A. Martinez, P. P. Provencio, S. T. Picraux, J. P. Sullivan, and B. S. Swartzentruber, J. Appl. Phys. **110**, 074317 (2011).
[18] D. A. Broido, M. Malorny, G. Birner, N. Mingo, and D. A. Stewart, Appl. Phys. Lett. **91**, 231922 (2007).
[19] N. Mingo, L. Yang, D. Li, and A. Majumdar, Nano Lett. **3**, 1713 (2003).
[20] J. Callaway, Phys. Rev. **113**, 1046 (1959).
[21] M. G. Holland, Phys. Rev. **132**, 2461 (1963).
[22] M. Asen-Palmer, K. Bartkowski, E. Gmelin, M. Carona, A. P. Zhernov, A. V. Inyushkin, A. Taldenkov, V. I. Ozhogin, K. M. Itoh, and E. E. Haller, Phys. Rev. B **56**, 9431 (1997).
[23] D. T. Morelli, J. P. Heremans, and G. A. Slack, Phys. Rev. B **66**, 195304 (2002).
[24] M. Kazan, S. Pereira, J. Coutinho, M. R. Correia, and P. Masri, Appl. Phys. Lett. **92**, 211903 (2008).
[25] M. Kazan, S. Pereira, M. R. Correia, and P. Masri, Phys. Rev. B **77**, 180302(R) (2008).
[26] H. B. G. Casimir, Physica **5**, 495 (1938).
[27] N. Mingo, Phys. Rev. B **68**, 113308 (2003).
[28] M. Kazan, G. Guisbiers, S. Pereira, M. R. Correia, P. Masri, A. Bruyant, S. Volz, and P. Royer, J. Appl. Phys. **107**, 083503 (2010).
[29] M. Kazan and S. Volz, J. Appl. Phys. **115**, 073509 (2014).
[30] M. Kazan, E. Moussaed, R. Nader, and P. Masri, Phys. Status Solidi C **4**, 204 (2007).
[31] G. Chen, Phys. Rev. B **57**, 14958 (1998).
[32] A. Balandin and K. L. Wang, Phys. Rev. B **58**, 1544 (1998).
[33] G. P. Srivastava, *The Physics of Phonons* (Hilger, Bristol, 1990).
[34] P. Reddy, K. Castelino, and A. Majumdar, Appl. Phys. Lett. **87**, 211908 (2005).
[35] M. Kazan, J. Heat Transfer **133**, 112401 (2011).
[36] M. Kazan, A. Bruyant, P. Royer, and P. Masri, Surf. Sci. Rep. **65**, 111 (2010).
[37] B. Latour, S. Volz, and Y. Chalopin, Phys. Rev. B **90**, 014307 (2014).
[38] R. Ortavy, Ann. Phys. **374**, 745 (1913).
[39] B. A. Aud, *Acoustic Fields and Waves* (Wiley, New York, 1973).
[40] N. Bannov, V. Aristov, V. Mitin, and M. A. Stroscio, Phys. Rev. B **51**, 9930 (1995).
[41] J. Zou and A. Balandin, J. Appl. Phys. **89**, 2932 (2001).
[42] E. P. Pokatilov, D. L. Nika, and A. Balandin, Superlattices Microstruct. **33**, 155 (2003).
[43] E. Pokatilov, D. L. Nika, and A. A. Balandin, Phys. Rev. B **72**, 113311 (2005).
[44] E. P. Pokatitilov, D. L. Nika, and A. A. Balandin, Superlattices Microstruct. **38**, 168 (2005).
[45] A. AlShaikhi and G. P. Srivastava, Phys. Rev. B **76**, 195205 (2007).
[46] Z. Alameh and M. Kazan, J. Appl. Phys. **112**, 123506 (2012).
[47] D. G. Cahill, F. Watanabe, A. Rockett, and C. B. Vining, Phys. Rev. B **71**, 235202 (2005).
[48] A. Ward and D. A. Broido, Phys. Rev. B **81**, 085205 (2010).
[49] B. Abeles, Phys. Rev. **131**, 1906 (1963).
[50] J. Grag, N. Bonini, B. Kozinsky, and N. Marzari, Phys. Rev. Lett. **106**, 045901 (2011).
[51] S. Moon, M. Hatano, M. Lee, and C. P. Grigoropoulos, Int. J. Heat Mass Transfer **45**, 2439 (2002).
[52] B. L. Zink, R. Pietri, and F. Hellman, Phys. Rev. Lett. **96**, 055902 (2006).
[53] J. Fang, C. Reitz, T. Brezesinski, E. J. Nemanick, C. B. Kang, S. H. Tolbert, and L. Pilon, J. Phys. Chem. C **115**, 14606 (2011).

17 April 2024 07:46:39